Non-Invasive Functional Evaluation of the Human Spinal Cord by Assessing the Peri-Spinal Neurovascular Network With Near Infrared Spectroscopy

Felipe Valenzuela, Mohit Rana, Ranganatha Sitaram, Sergio Uribe, and Antonio Eblen-Zajjur

***Abstract*— Current medical care lacks an effective functional evaluation for the spinal cord. Magnetic resonance imaging and computed tomography mainly provide structural information of the spinal cord, while spinal somatosensory evoked potentials are limited by a low signal to noise ratio. We developed a non-invasive approach based on near-infrared spectroscopy in dual-wavelength (760 and 850 nm for deoxy- or oxyhemoglobin respectively) to record the neurovascular response (NVR) of the peri-spinal vascular network at the 7th cervical and 10th thoracic vertebral levels of the spinal cord, triggered by unilateral median nerve electrical stimulation (square pulse, 5-10 mA, 5 ms, 1 pulse every 4 minutes) at the wrist. Amplitude, rise-time, and duration of NVR were characterized in 20 healthy participants. A single, painless stimulus was able to elicit a high signal-to-noise ratio and multi-segmental NVR (mainly from Oxyhemoglobin) with a fast rise time of 6.18 [4.4-10.4] seconds (median [Percentile 25-75]) followed by a slow decay phase for about 30 seconds toward the baseline. Cervical NVR was earlier and larger than thoracic and no left/right asymmetry was detected. Stimulus intensity/NVR amplitude fitted to a 2nd order function. The characterization and feasibility of the peri-spinal NVR strongly support the potential clinical applications for a functional assessment of spinal cord lesions.**

***Index Terms*— fNIRS, functional test, nerve stimulation, neuro-vascular coupling, neuro-vascular response, spinal cord.**

Manuscript received February 5, 2021; revised June 7, 2021, July 28, 2021, and September 19, 2021; accepted October 5, 2021. Date of publication October 27, 2021; date of current version November 10, 2021. The work of Felipe Valenzuela was supported by the Scholarship under Grant Comisión Nacional de Investigacion Cientifica y Tecnologica (CONICYT)-21171608. The work of Mohit Rana and Ranganatha Sitaram was supported in part by the Comisión Nacional de Investigacion Cientifica y Tecnologica (CONICYT) through the Fondo Nacional de Desarrollo Cientifico y Tecnológico (Fondecyt) Post-Doctoral Grant under Grant 3100648, in part by the Fondecyt Regular under Project 1171313 and Project 117132, and in part by the CONICYT Programa de Investigación Asociativa (PIA)/Anillo de Investigación en Ciencia y Tecnología under Grant ACT172121. The work of Sergio Uribe and Antonio Eblen-Zajjur was supported in part by the Fondo de Fomento al Desarrollo Cientifico y Tecnologico (FONDEF) under Grant ID18I0064, in part by the Fundación COPEC-UC under Grant 2018R.1030, in part by the Global-UC under Grant 2018-IV, and in part by the Patentar-Pontificia Universidad Católica de Chile under Grant 2018-DTD-UC. *(Corresponding author: Antonio Eblen-Zajjur.)*

This work involved human subjects or animals in its research. Approval of all ethical and experimental procedures and protocols was granted by the Pontificia Universidad Católica de Chile Comisión Ética-Científica under Protocol No.: PUC-170914003, October-2017.

Felipe Valenzuela is with the Center for Biomedical Imaging, Pontificia Universidad Católica de Chile, Santiago 6513677, Chile (e-mail: fgvalenzuela@uc.cl).

Mohit Rana is with the Division of Neuroscience, Department of Psychiatry, School of Medicine, Pontificia Universidad Católica de Chile, Santiago 6513677, Chile (e-mail: makrana85@gmail.com).

Ranganatha Sitaram is with the Diagnostic Imaging Department, Multimodal Functional Brain Imaging and Neurorehabilitation Hub, St. Jude Children's Research Hospital, Memphis, TN 38105 USA (e-mail: ranganatha.sitaram@stjude.org).

Sergio Uribe is with the Millenium Nucleus for Cardiovascular Magnetic Resonance and the Radiology Department, School of Medicine, Pontificia Universidad Católica de Chile, Santiago 6513677, Chile (e-mail: suribe@uc.cl).

Antonio Eblen-Zajjur is with the Translational Neuroscience Laboratory, Facultad de Medicina, Universidad Diego Portales, Santiago 8370109, Chile (e-mail: antonio.eblen@udp.cl).

Digital Object Identifier 10.1109/TNSRE.2021.3123587

I. Introduction

THE spinal cord is a frequent target of traumatic, degenerative, tumoral, compressive, or vascular lesions, but is also involved in neuropathic pain [1]. Every year, up to 500,000 people suffer a spinal cord injury, affecting the most productive ages of life [1], additionally, up to half of the adult population suffers symptomatic spinal hernia [2]. Currently, there is a relative lack of functional assessment of the spinal cord which contrasts to the well-developed structural evaluation by Magnetic Resonance Imaging (MRI) or Computed Tomography techniques [3]. Functional MRI (fMRI) that measure the Blood Oxygenation Level-Dependent signal (BOLD), arterial spin labeling, and diffusion-weighted imaging, have been successfully used to detect brain cortical activation areas associated with cognitive, sensory, or motor activity. However, the clinical application of these techniques to the spinal cord remains challenging due to the small cross-section areas, strong motion artifacts, low signal-to-noise ratio, and inhomogeneities produced in areas near the spinal cord [4]–[11]. The spinal cord BOLD signal activation has been recorded at the corresponding spinal segment applying peripheral sensory stimulation in noxious intensity ranges [5], [7] or by long-lasting finger-tapping motor tasks [6]. Despite these paradigms, resulting BOLD signals showed low amplitudes compared with the baseline signal [5], [7]. Recent developments are gradually overcoming these challenges and increasing the potential clinical applications [8]–[11].

This work is licensed under a Creative Commons Attribution 4.0 License. For more information, see https://creativecommons.org/licenses/by/4.0/

A functional evaluation of the spinal cord can be performed using motor (MEP), somato-sensory (SEP), and spinal evoked potentials (SSEP), giving relevant information about spinal inter-neuronal electrical response [12]. However, SSEP recorded from skin electrodes shows a low signal-to-noise ratio, requiring several (>500) stimuli for signal averaging [12]–[14]. Nevertheless, such stimulation increases the risk for potentiation, sensibilization [13]–[14], discomfort, or pain [12]. Invasive electrodes placed directly at the spinal cord result in a better signal-to-noise-ratio, but reduces its clinical use to monitoring the spinal cord during surgery [15]. Focal spinal lesion associated with mild symptoms like paresthesia or paresis, generally shows few SSEP signs, if any [12].

Brain Functional Near-Infrared Spectroscopy (fNIRS) uses the propagation of the infrared light through tissues until the brain cortex undergoing absorption mainly induced by oxyhemoglobin (HbO_2) and deoxyhemoglobin (Hb) [16]. Increased neuronal activity is linked to regional vasodilation, augmented blood flow, and changes of HbO_2 and Hb concentrations recorded by fNIRS [17], [18].

Animal studies in which fNIRS have been applied invasively, support the notion that this technique could be relevant for spinal cord monitoring during regional surgery, detection of spinal cord injuries, and to follow up therapeutic interventions for spinal lesions [19]. Even more, human intraoperative studies suggest that the spinal neurovascular response (NVR) is modified by spinal cord ischemia supporting its use for human spinal cord monitoring [15].

In this work, we hypothesized that the electrical stimulation of a peripheral nerve will induce an increased neuronal activity at the spinal dorsal horn (SDH) triggering a vasodilation that spreads from the spinal cord to the peri-spinal vascular network [15], allowing a non-invasive fNIRS system to detect HbO_2 and Hb changes as a part of the NVR that could be used as an evaluation and monitoring of the human spinal cord function.

II. Method

A. Participant Recruitment

The experimental protocol was approved by the ethics committee at Pontificia Universidad Católica de Chile (PUC-170914003, 2017). The study involved apparently healthy participants after their written informed consent. A total of 20 healthy participants agreed to be included in the study, gender distribution was 6 females (30%) and 14 males (70%), with an age range from 22 to 57 years old (26 [25-28.7]; median [25-75 Percentiles]). Body mass index (BMI) range was from 21 to 30 (26.03 [22.7-27.3]).

B. Device for Recording the Spinal NVR Triggered by Electrical Stimulation of the Median Nerve

Spinal NVR was triggered by electrical stimulation of the left median nerve, using a bipolar transcutaneous electrical stimulator (WPI-A310™; cathode proximal and 3 cm from anode) applied on the skin using electroconductive gel, over the nerve at the wrist medial midline (Fig. 1 left). The ground electrode was placed at the dorsal face midpoint of the same forearm. Each electrical stimulus had a constant current that ranged from 5 to 10 mA, and a duration of 5 ms monophasic square pulse. The pulse duration was selected after a systematic test of a 0.1 to 5 ms range to achieve just the maximal NVR amplitude. These stimulus characteristics induce a clear but painless sensation and a low to moderate medial fingers jerk.

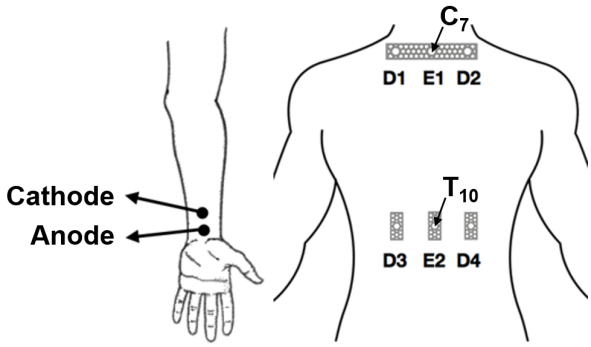

Fig. 1. Non-invasive placement of the optodes at C7 and T10 levels (right side). E1 and E2: cervical and thoracic infrared sources placed at spinous process of C7 and T10 respectively; D1and D2: left and right infrared cervical detectors at 4.5 cm each from the emitter; D3 and D4: left and right infrared thoracic detectors at 4.5 cm each from emitter. Left: Peripheral median nerve electrical stimulation site at the wrist using a bipolar skin surface electrode (cathode proximal; separated 3cm from the anode).

Stimulus intensity of up to 3 times the sensory threshold was able to elicit adequate spinal NVR, which is similar to the stimulus intensities used for somatosensory evoked potentials. Since stimulating intensities in the order of 10 mA could be uncomfortable to some participants, all of them were informed about this possibility and a visual analog scale for pain intensity was obtained.

C. Positioning Vertebral Optodes

Simultaneous NVR from two different spinal cord regions elicited by the same stimuli were studied. Signals from the surrounding tissues at the cervical and lumbar level were recorded by placing optodes holders at the vertebral spinous process of the C7 and T10 respectively using clinical non-allergic adhesive strips over isopropyl alcohol cleaned skin. These optode locations were selected because of their close location to spinal cord sensory cervical and lumbar enlargements (Fig. 1 right) that means that in the present study the NVR recorded at T10 will be reported as lumbar to match spinal cord segment. At each level, the source optode was placed at the midline position (E1 and E2, Fig. 1 right) with a detector optode on both sides (D1 and D2 for cervical, D3, and D4 for thoracic levels, Fig. 1 right). In all cases, the source-detector separation was fixed at 4.5 cm. This distance was found to give the deepest recorded NIR signal at the best signal-to-noise-ratio based on the different emitter-detector distances from 1 to 6 cm in 5 mm steps that were tested, shorter or larger than this distance resulted in a significant reduction of the recorded NVR amplitude. Special optode holders placed at the patient's back were designed and 3D-printed. The result was two types of holders: the cervical holder able to hold

three optodes horizontally (one emitter and two detectors), and three individual optode holders for the thoracic level (Fig. 1 right). The detailed description of the entire device can be found in a recent patent application [20]. Magnetic resonance imaging of the vertebral column, using T1, T2, and STIR MRI sequences were acquired in 3 participants to confirm the correct anatomical placement of the optodes, considering the thickness of vertebral structures, amount of adipose tissue, and musculature.

D. fNIRS Data Acquisition

Spinal NVRs were recorded using a commercially available fNIRS device (NIRx Optical Neuroimaging System™, Germany) designed for brain fNIRS and based on a continuous wave technology. The system uses a time-multiplexed method to combine sources and detectors without interference, with dual wavelengths of 760 nm and 850 nm i.e., under and above hemoglobin spectral isosbestic point within <1 pW sensitivity.

E. Experimental Setup

Each volunteer was informed about the test, then instructed to lie down in a prone position on a massage bed with the face inside the window of the bed in a quiet room and dimmed lighting. The optode holders were placed as described above. In 4 patients, small diameter adhesive electrodes for electromyographic (EMG) recording were also placed at the skin close to detection optodes. In 3 other participants, the optodes were placed horizontally over the ipsilateral subscapular area for fNIRS recording far away from the spinal cord.

F. Experimental Protocol

Three protocols were used to characterize the NVR to peripheral electrical nerve stimulation: a) Intensity-Response relationship: Three stimuli at 5, 7.5, or 10 mA intensities respectively were applied with a 4 minutes interstimulus interval (ISI); b) Long inter-stimulus interval (Long-ISI): A sequence of three stimuli at 10 mA intensity was given with 4 minutes of ISI. This low-frequency stimulation was selected to prevent spinal cord phenomena related to potentiation, habituation, or refractoriness; c) Short inter-stimulus interval (Short-ISI): To evaluate the possible link between spinal triggered NVR to peripheral nerve stimulation and spinal phenomena related to potentiation, habituation, or refractoriness, five stimuli were applied separated by 1 minute. At the end of each protocol, participants were asked to quantify the subjective intensity of stimulation by using the visual analog scale (VAS).

G. Data Processing and Analysis

Raw optical density values for each experiment were saved in plain text files for further offline processing: a) Filtering: The stimulus flag was used as a start mark for the time series analysis. A shift-invariant 6-th order IIR-Butterworth filter with cut frequencies at 0.2 Hz, in both the forward and reverse directions, based on 31.25 Hz sampling rate, was applied to get rid of low-frequency signals, and some attenuation for high-frequency signals. Four level wavelet denoising was used to filter the remaining noise. Finally, the detrending of the data was applied to remove the effects of any systematic drift and, b) Reconstruction and normalization: Filtered raw optical intensities were processed using the modified Beer-Lambert law (MBLL) to obtain HbO_2 and Hb concentrations expressed in $mmol{\cdot}L^{-1}$. The signal from each source-detector pair was reconstructed separately. The four signals (Left/Right/C7/T10) were normalized and centered around the mean of the baseline one second before the stimulus.

H. Quantitative and Statistical Analysis

NVR was continuously recorded; a stimulus flag was used to analyze the NVR wave quantitatively. The NVR was characterized by its rise time (from stimulus flag to maximal peak), peak amplitude, and duration (full width at half-maximum [FWHM]), and described using distribution-free statistics. A mixed statistical model including both, the fixed but also random effects were assumed. A comparison of two groups was performed using a paired, non-parametric, two-tailed Mann-Whitney U test (MW). Linear and non-linear regressions were estimated between stimulus intensity and NVR parameters. Spearman non-parametric rank-order correlation coefficient rs was calculated for BMI and spinal fNIRS parameters but also for these parameters and stimulus intensity values. The significance level was set at $p < 0.05$ for all tests.

III. Study Results

A. General Characteristics of Nerve Stimulation Induced-Spinal NVR

A single electrical pulse (5 to 10 mA) applied unilaterally to the median nerve elicited a full NVR at both (C7 and T10) levels. In the majority of the participants, maximal stimulus intensity (10mA) was able to induce a light distal jerk of 1 to 3 median fingers. VAS value was 2 [2-3.75] (median [25-75 percentile]) for a 0 to 10 scale, only one (1/20) patient reported the 10 mA stimulation for VAS = 7.

An average from 3 NVR (Fig. 2) shows a robust response with low dispersion. The onset of the NIRS signal occurs after about 3 seconds delay showing a fast rise time of 6.18 [4.4-10.4] seconds (median [Percentile 25-75]) followed by a slow decay phase for about 30 seconds toward the baseline. This was observed for the HbO_2, but about one order of magnitude lower for the Hb (Fig. 2), therefore the subsequent statistical analysis was performed for the HbO_2 exclusively. The average NVR from the 20 healthy participants obtained from the long-ISI protocol is presented in Fig. 2. Cervical responses show higher HbO_2 concentration values (+7.95% $p<0.01$; Table I, Figs. 2 and 3) and shorter rise time than thoracic responses (−17.0%; $p<0.01$; Table I, Figs. 2 and 3).

B. Absence of Left/Right Spinal NVR Asymmetry in Normal Participants

Although the spinal cord NVR were elicited by unilateral (left) median nerve stimulation, comparison between left and right responses (Table II and Fig. 2) did not show significant differences in amplitude at C7 nor T10, in rise

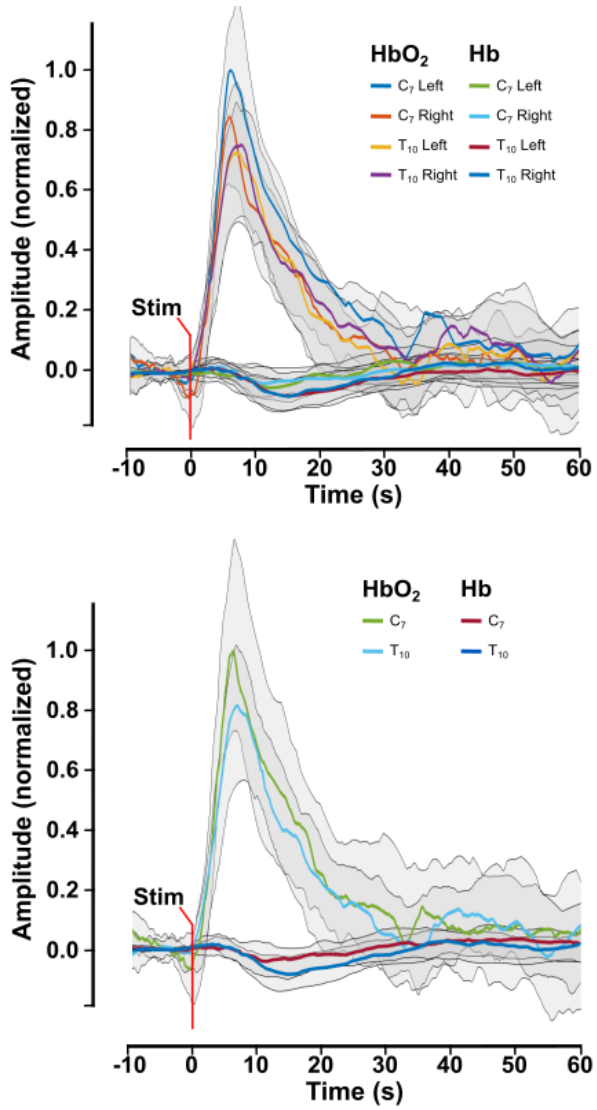

Fig. 2. Spinal NVR from 20 different healthy participants, elicited by left median nerve electrical stimulation applied at time 0. Curves are averaged responses (n=3 from each volunteer). HbO_2 responses are higher than the near-zero Hb responses. Upper panel: patterns from Left/Right and C7/T10 recording sites. No significant difference was detected between Left/Right values neither at C7 nor T10. Lower panel: Left/Right pooled data to compare C7 and T10 recording sites. HbO_2 C7 amplitude was significantly higher than the T10 value. No significant differences were found among Hb responses from C7 and T10. Curves are median (colored) with 25-75 percentiles (grey).

time at C7 nor T10, and in the duration of the response at C7 nor T10. After these results, left/right side measurements were pooled together and n measurement values were 40.

C. Nerve Stimulation-Induced Spinal NVR Did Not Depend on Local Muscular Activity nor Vascular Skin Response

Spinal NVR at C7 level was simultaneously recorded with EMG activity using surface electrodes placed in close contact to the fNIRS detector optodes at the medial upper area of the trapezius, rhomboid minor, and lower area of splenius capitis muscles. No local EMG activity was observed by the peripheral median nerve electrical stimulation, either by a single pulse at the highest verified intensity (10 mA; Fig. 4) or with trains of 7, 13, or 25 pulses applied at 5Hz (Fig. 4). Even voluntary contractions strong enough to extend the neck over the horizontal line did not induce significant fNIRS changes (Fig. 4). Optodes array placed at the ipsilateral subscapular area were able to detect heartbeats but not any vascular response to the maximal intensity i.e., 10 mA of repeated median nerve stimulation during long-ISI protocol (Fig. 5).

TABLE I
DIFFERENTIAL NVR BETWEEN CERVICAL (C_7) AND THORACIC (T_{10}) FOR AMPLITUDE, RISE TIME, AND DURATION (FWHM) PARAMETERS OF SPINAL RECORDED NIRS SIGNALS INDUCED BY LEFT MEDIAN NERVE ELECTRICAL STIMULATION

	%	$U_{40,40}$	z	p
Amplitude (n.u.)	+6.1	526	-2.63	<0.01
Rise Time (s)	-17.0	459.5	-3.27	<0.001
FWHM (s)	n.s.	674	-1.2	n.s.

Percentage of change of cervical to thoracic signal (+ means C7 larger; - means C7 smaller); n.u. = normalized values; FWHM = full width at half-maximum; $U_{n1,n2}$: Mann-Whitney U(samples); z value; p: significance

TABLE II
SPINAL LEFT/RIGHT RECORDINGS COMPARISON OF SPINAL CERVICAL (C_7) AND THORACIC (T_{10}) NVR ELICIT BY LEFT UNILATERAL MEDIAN NERVE ELECTRICAL STIMULATION FOR AMPLITUDE, RISE TIME, AND DURATION (FWHM) PARAMETERS

	Level	$U_{20,20}$	z	p	
Amplitude:	C7	181	-0.5	0.6	n.s.
	T10	190	-0.2	0.8	n.s.
Rise time:	C7	170	-0.8	0.4	n.s.
	T10	195	-0.1	0.9	n.s.
FWHM:	C7	190	-0.2	0.8	n.s.
	T10	196	-0.09	0.9	n.s.

n.s. non-significative; FWHM = full width at half-maximum; $U_{n1,n2}$: Mann-Whitney U (samples); z value; p: significance

D. Influence of Body Mass Index on NVR Values

Correlation analysis between BMI and NVR parameters showed non-significant association under our experimental setup, for NVR amplitude (rs=0.05; p>0.05); rise time (rs=0.1; p>0.05) or duration (rs=0.07; p>0.05).

E. Peripheral Nerve Long- and Short-ISIs Modify Spinal NVR

Increased stimulation frequency from one pulse every 4 minutes to one pulse per minute reduced NVR amplitude at the cervical level (−8.4%, $p < 0.05$) but not at the thoracic

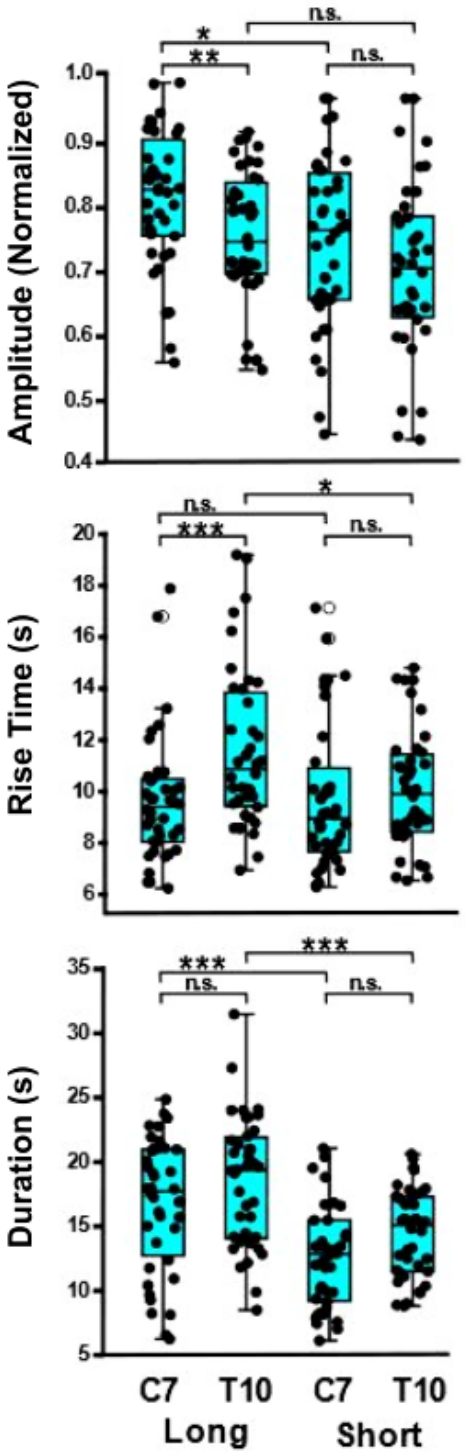

Fig. 3. Median (center horizontal lines inside the box), 25-75 percentiles (box) and minimal and maximal values (whiskers) for relative amplitude, rise time and duration (full width at half-maximum: FWHM) of NVR recorded at C7 and T10, triggered by long- or short-inter-stimulus interval electrical stimulation at the left median nerve. *** = $p < 0.001$; ** = $p < 0.01$; * = $p < 0.05$; n.s. = non-significant.

level (Table III and Fig. 3). The rise time of the NVR did not change at the cervical level, but it did at the thoracic level and was shorter than that observed during short-ISIs (−13.3%, Table III and Fig. 3). The duration of spinal NVR shows a reduction by 21.4% at the cervical level and a reduction by

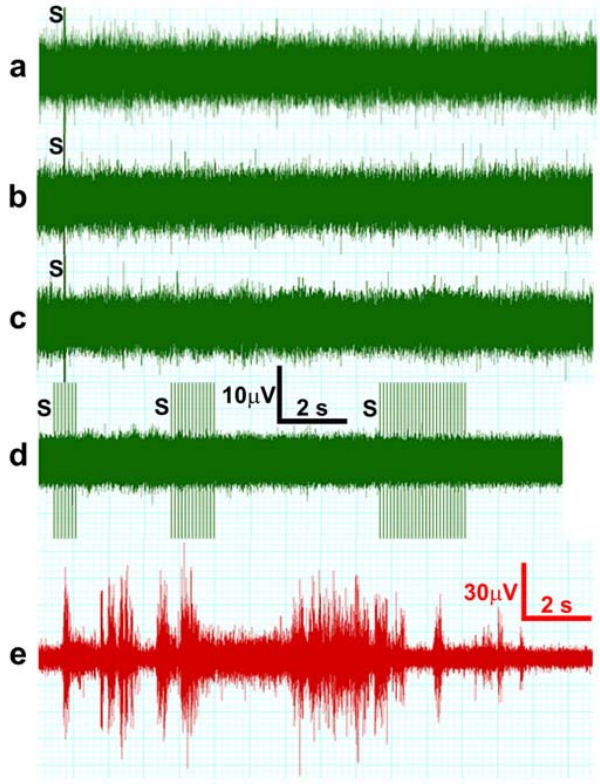

Fig. 4. Spinal NVR at C7 level simultaneously recorded with surface electromyography (EMG) from medial upper area of the trapezius. The trapezius EMG activity subjacent to the cervical optodes was recorded before and after median nerve single electrical pulse stimulation (traces a to c). Stimulus artifact is marked as S. Three different stimulus intensities were tested i.e., 5 (trace a), 7.5 (trace b), and 10 mA (trace c). None of these stimuli was able to induce EMG activity. Even a train of 7, 13, or 25 electrical pulses at 5 Hz (trace d) applied to the median nerve at the wrist was not able to activate EMG activity close to fNIRS optode. Voluntary contractions of extensor muscles of the neck were recorded by EMG in the same volunteer (trace e) showing no correlation between NVR and EMG even during maximal voluntary neck extension.

TABLE III
EFFECT OF PERIPHERAL MEDIAN NERVE SHORT-ISIS ON SPINAL NVR FOR AMPLITUDE, RISE TIME, AND DURATION (FWHM)

	Level	%	$U_{40,40}$	z	p
Amplitude (n.u.)	C_7	-8.4	564	-2.26	< 0.05
	T_{10}	n.s.	609	-1.83	> 0.05
Rise Time (s)	C_7	n.s	765	-0.33	> 0.05
	T_{10}	-13.3	565	-2.25	< 0.05
FWHM (s)	C_7	-21.4	431	-3.55	< 0.001
	T_{10}	-21.8	412	-3.73	< 0.001

Percentage of change from long-ISI values; n.u. = normalized values; FWHM = full width at half-maximum; n.s. =non-significant; $U_{n1,n2}$: Mann-Whitney U(samples); z value; p: significance.

21.8% at the thoracic level for long-ISIs values (Table III and Fig. 3). No left/right asymmetries were found during short-ISIs stimulation.

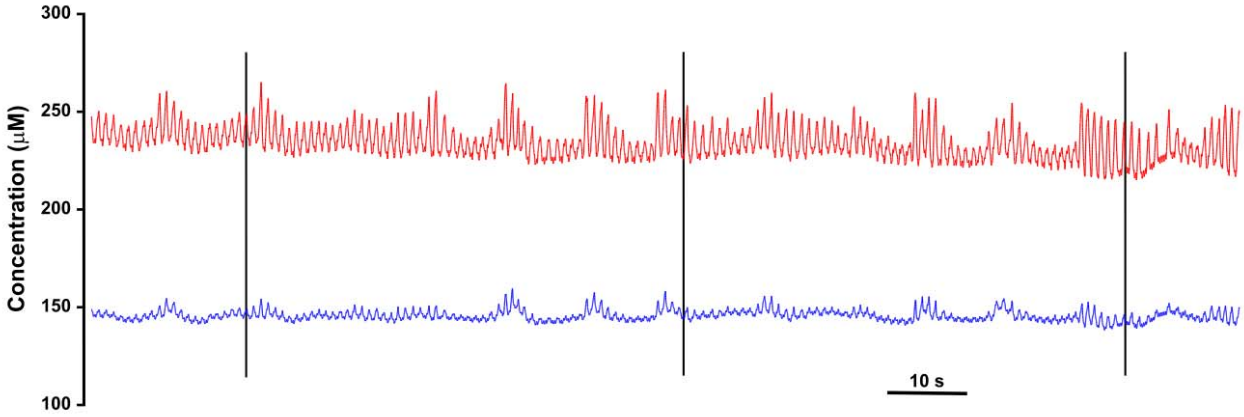

Fig. 5. fNIRS signals recorded at ipsilateral subscapular area during left median nerve electrical stimulation at the wrist. HbO_2 (red) and Hb (blue) concentrations (μM) are shown. Black vertical flags correspond to three single, 5 ms, 10 mA square electrical pulses applied to the median nerve at 1 pulse every 4 minutes following long-ISI protocol. Background activity shows heartbeats within oscillations of the baseline. None of these stimuli was able to induce neither skin nor muscle vascular responses.

TABLE IV
STIMULUS INTENSITY-SPINAL NVR RELATIONSHIPS FOR AMPLITUDE (N.U.), RISE TIME (S), AND DURATION (FWHM IN SECONDS) PARAMETERS OF CERVICAL AND THORACIC NIRS SIGNALS ELICITED BY LEFT MEDIAN NERVE ELECTRICAL STIMULATION

	Level	*rs*	*F*	*p*	**Regression equation**
Amplitude	C7	0.44	11.2	10^{-6}	$-0.00135X^2 + 0.047X + 0.43$
	T10	0.38	7.6	10^{-5}	$-0.00158X^2 + 0.049X + 0.39$
Rise time	C7	0.02	0.04	0.8	n.s.
	T10	0.06	0.44	0.5	n.s.
FWHM	C7	0.25	4.17	10^{-3}	$-0.028X^2 + 1.002X + 8.65$
	T10	0.21	7.40	0.02	$-0.145X^2 + 3.242X + 0.88$

rs: Spearman´s coefficient of correlation; *F:* Fisher; *p*: significance; n.s.: non-significant; FWHM = full width at half-maximum.

F. The Stimulus Intensity-Response Relationship Follows a Second-Order Function

Progressive increases in the stimulation intensity of the median nerve induced an increase in the amplitude and duration of the spinal NVR recorded at both cervical and thoracic levels but, non-significant changes were detected for the rise time at any recorded place (Table IV and Fig. 6). A nonlinear second-order relationship for amplitude and duration variables was observed for NVR to increasing stimulus intensity (Fig. 6 and Table IV for curve fitting values). The maximum stimulus intensity tested (10 mA) did not reach the amplitude plateau for the cervical NVR in contrast to the thoracic response (Fig. 6).

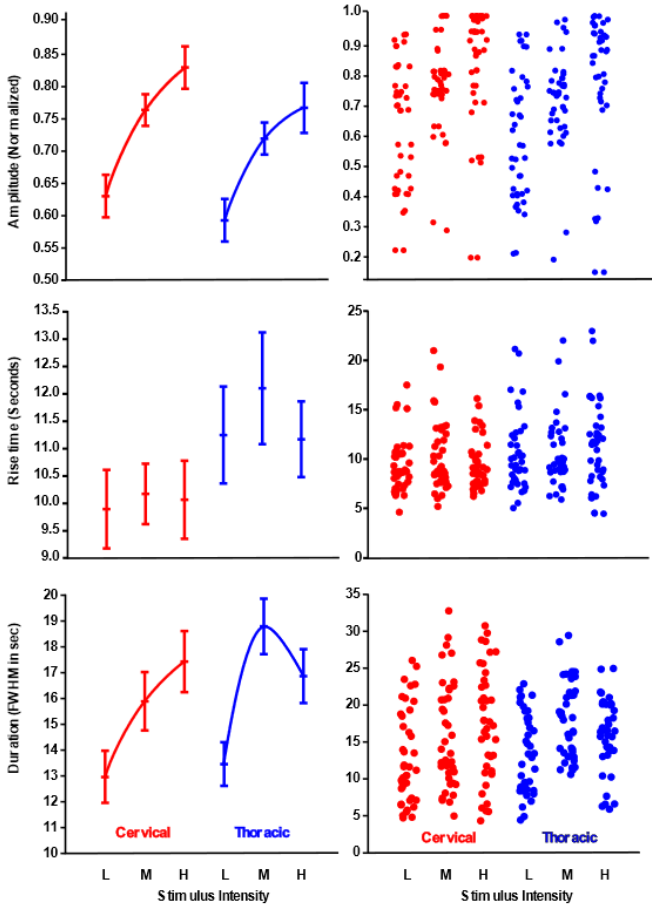

Fig. 6. Stimulus intensity-NVR relationship obtained from cervical (C7; red) and thoracic (T10; blue) spinal recording sites and median nerve electrical stimulation at Low (5mA), Medium (7.5 mA), or High (10 mA) currents. Median and 25-75 percentiles (left) and jitter diagrams (right) for amplitude, rise time, and full wave at half maximum (FWHM) duration parameters. See Table IV for correlation/regression analysis. Only significant curve fitting functions are shown ($p < 0.05$).

IV. DISCUSSION

A. General Findings

In the present study, the spinal NVR triggered by the unilateral median nerve electrical stimulation was recorded in 20 healthy participants for the first time, by a non-invasive fNIRS system. A single electrical pulse applied unilaterally to the median nerve was able to elicit a full NVR at both C7 and T10) mainly based on HbO_2 signal, returning to baseline values after around 30 seconds. The recorded spinal

NVR did not depend on local muscular activity. No left/right asymmetry was found for spinal NVR in healthy participants, with larger amplitude at cervical compared to the thoracic spinal level. The amplitude of Spinal NVR depends on the intensity and frequency of the nerve stimulation. The higher amplitude of the HbO_2 over the Hb signal agrees with those reports where brain cortex HbO_2 values are circa 33% larger than Hb [21].

B. Characteristics of the Peri-Spinal NVR Triggered by Peripheral Nerve Stimulation

Median nerve stimulation activates mainly C7 to C8 segments of the spinal dorsal horn. The incoming afferent volleys along the spinal root, SDH inter-neuronal activity, and the primary afferent depolarization processes take place leading to neuronal synchronization [22]–[24]. We apply pulse width longer than nerve chronaxie to reduce the impact of overlapping factors such as skin resistance, amount of subcutaneous fat, edema, inflammation, ischemia but also nerve degeneration or denervation, which affect the nerve excitability and the spinal cord input. This pulse duration minimizes stimulus power at the threshold, and distribute the stimulus more homogeneously for short to large fibers [25]. During preliminary tests, 1 ms pulse fails to induce spinal NVR in more than 75% of the cases.

C. Neuro-Vascular Coupling in the Spinal Cord

Spinal dorsal horn sensory neurons show strong synchronous discharges induced by common inputs from primary afferents [22]. The nerve stimulation increases spinal neuronal metabolism, enzymatic activity and oxygen consumption [26], [27]. Neurons release glutamate which activates astrocytic mGluR2/3/5 receptors [28], arachidonic acid cascade [13], [28]–[30], cyclooxygenases (COXs) activity and E2 prostaglandin release inducing local vasodilation and increased regional blood flow.

Vasodilation spreads throughout the peri-spinal vascular net by the smooth muscle functional syncytium and gap junctions [28]–[30], [31] to both up- and downstream directions from the active regions [32], [33]. The spinal cord is localized about 5-6 cm depth from the skin and the penetration depth of the fNIRS implemented is about 2-2.5 cm [34]. This fact strongly supports the notion that the main source of the recorded fNIRS signal is the more superficially spreading peri-spinal NVR [15] consequence of the activation of the spinal cord through the electrical stimulation of the peripheral nerve. Furthermore, we demonstrated that even during the local neck and upper back muscle tonic or phasic contractions tested by EMG were unable to trigger deep fNIRS responses. Contribution of the skin and nearby muscle activity to the fNIRS signals would be marginal. The contribution of the tissular fat to the NVR signal was indirectly tested applying correlation analysis between BMI and NVR parameters, i.e., rise time, amplitude, or duration, showing non-significant association under our experimental setup. Therefore, adipose tissue and bone had negligible effects in the recorded spinal NVR.

D. Other Potential Source of NVR

Sympathetic Skin Response has been reported to participate in brain fNIRS responses [35] however, such contribution is generated by noxious stimulation (VAS$\geq$7/10) which triggers both superficial skin (detected by shortly separated optodes) and brain response (recorded by long separated optodes). Our experimental setup applies non-noxious stimulation which excludes sympathetic skin responses but additionally, the long emitter-detector distance (4.5 cm) mainly detects signals deeper beyond the skin [34] reducing drastically the signal contribution from the skin.

Noxious mechanical stimulation of the skin can induce an increase of the spinal cord blood flow by increased arterial blood pressure and by spinal cord neuronal activation [36] but, spinal NVR reflect neuronal activity even when large fluctuations in blood pressure occur [37]. The median nerve electrical stimulation was self-reported as painless, additionally, our stimulation protocol was unable to increase the mean blood pressure.

E. No Left/Right Peri-Spinal NVR in Healthy Subjects

The spinal NVR spreads bilaterally despite the unilateral median nerve stimulation, with no statistical difference in amplitude, rise time, and duration when recorded at either side of the same vertebral level. Several explanations should be considered. The first, the functional syncytium of the peri-spinal vascular net (*vide supra*), the second, the well-known inter-spinal dorsal horn connections through arcuate fibers [13], the third, long temporal curse of NVR but, the fourth, potential side asymmetry of the NVR in patients with hemi-section or other unilateral spinal lesions could be expected.

F. Multi-Segmental NVR

The fact that median nerve stimulation elicits the NVR at cervical but also lumbar levels, can be explained by the spinal intersegmental modulation but also by the intraspinal and supraspinal connectivity [13], [24], [38]. The tonic descending modulation originated at supraspinal structures such as periaqueductal gray, locus coeruleus, rostroventral brainstem [13], [39] is a well-known source of all spinal segment afferences whose modulation could be changed by non-noxious stimulation [40].

Descending diffuse noxious inhibitory controls (DNIC) from the brainstem reticular formation [40] as well other spinal intersegmental modulations [13], [24], [38], should not be involved because the stimulus intensity should be in the noxious range to trigger the modulation. Experimental data showed that electrical stimulation of the oral trigeminal area with cervical input, induces robust cord dorsum evoked potentials at the lumbar segment [41] and modification of lumbar reflex [42]. All these facts support the notion of a multiple, simultaneous (excitatory but also inhibitory) and dynamic descending modulation to all spinal segments [5], [39] with stimulus-induced changes, even to non-noxious stimulation [43] potentially involved in the spinal NVR recorded in the present study at cervical and thoracic

levels to match the sensory enlargements of the spinal cord, however, other vertebral levels in between, display similar NVR to the median nerve electrical stimulation (data not shown).

Previous studies have shown that stimulus increased synchronization of SDH neuronal activity and spinal multisegmental modulation [13], [14], [24], [38] which is exerted by a longitudinally, bilaterally ensemble of functionally interconnected spinal neurons leading to a sensory modulation of the information transmitted by afferents to other segmental and supraspinal networks [22]–[24], [40], [44].

The spinal evoked potentials directly measure post-synaptic dorsal horn potentials [13], [22], [24], [38] on the other hand, fNIRS measures not only the dorsal horn response but also the neurovascular coupling process which are involved in several pathological processes.

The current optodes placement was chosen to increase potential detection of NVR asymmetry induced by unilateral spinal lesion i.e., traumatic hemi-section, unilateral compression, side gradient lesion, etc. We are currently testing different optodes arrays i.e., linearly vertical, rhomboidal with emitters at vertical vertices, etc., each of them could show differential sensitivity to the lesion location.

G. Short-ISI Stimulation Induces Reduction of the Peri-Spinal NVR

Spinal phenomena such as long-term depression (LTD) [45] is induced by lower neuronal depolarization, lower intracellular calcium increases, and lower stimulation frequency [45] than those required to induce long term potentiation (LTP) [13], [40]. It is well known that both LTD and LPT phenomena can be exhibited by SDH neurons which receive primary afferent synapses [13], [45], and that low-frequency stimulation i.e., 1 Hz, can induce LTD in neurons from the superficial SDH neurons [45]. The fact that increased stimulation frequency induced a reduction of duration at C7 and T10 levels, rise-time at T10, and amplitude at C7 of the NVR support the notion for the existence of LTD influencing the NVR.

H. Spinal Cord Descending Modulation

The longer rise time at T10 than at C7 can be explained by the fact that the median nerve stimulation activates a cervical, supraspinal, and descending spinal loop with diffuse modulatory effect [39] but requiring more time to reach the thoracic level. On the short-ISI protocol, we did not see this difference (Fig. 5) suggesting that the system, if excited too often, becomes potentiated in its responses. Similar behavior had been reported in cortex fNIRS of infants [35]. In contrast, the duration of spinal NVR is about the same for C7 and T10. This suggests that the response is stereotypically homogeneous at different metameres. In this regard, the decay phase of the spinal NVR was longer than the rise time which strongly suggests that: 1) a gradual reduction in the neuronal activity has occurred; 2) the return of neuronal and glial intracellular calcium to the rest concentration [28], [29] and, 3) a washout effect that reduces gradually the peri-vascular concentration of vasodilator agents has occurred.

I. Stimulus Intensity-Response Relationship

The amplitude of the NVR is directly related to the intensity of the stimulus. For spinal evoked potentials this phenomenon is well known [13], [14]. NVR amplitude was fitted to a logarithmic function showing a slowing down of the response at high stimulation intensity. This result agrees to the report that the BOLD response in the spinal cord shows linear properties for long-lasting stimuli duration (at least 21 s), whereas, for shorter stimulations, the amplitude of the signal differs from the linear model [6]. Similar nonlinearity has been reported in the brain to be generated from the neurovascular coupling process where a saturation of the neuronal activity on cerebral blood flow changes [6]. The fact that the maximum stimulus intensity tested (10 mA) was unable to reach a plateau for the cervical NVR could be due to the non-noxious intensity of the stimulation as shown a mean VAS value lower than 2.6/10. Higher stimulation intensities in the noxious range or long-lasting stimulation, probably will reach the amplitude plateau of the spinal NVR in a similar way as shown in fNIRS [6] electrophysiological [13], [14] but also by MRI-BOLD [5], [6], [7] techniques.

J. Spinal Origin of the NVR Triggered by Painless Peripheral Nerve Stimulation

Iso-potential mapping of the field potentials (N wave) generated within the spinal grey by non-noxious electrical stimulation of a cutaneous or mixed peripheral nerve reveals activation loci at Rexed's laminae IV-V of the dorsal horn coincident to Aα and Aβ fibers targets, additionally, the field potential reverses in sign in the ventral horn [46]. Several facts strongly suggest that the contribution of electrical antidromic activation or voluntary activation of the spinal motoneurons, to spinal NVR, when present, was marginal, i.e., a) the light motor response (tree fingers jerk) observed only at 10 mA (maximal intensity used); b) an intense voluntary motor task such as tightly closing of one hand for 60 s or 5 strong hand claps failed to trigger a spinal NVR (data not showed); c) in the cat experimental model, orthodromic stimulation of the dorsal root induced an average increase in spinal blood flow of 128% above control values, whereas, antidromic (ventral root) motoneuron activation failed to produce any significant changes in spinal blood flow [47]; and d) tactile stimulus-evoked BOLD signals covaried with electrophysiological recording of neuronal multiunit activity and local field potentials in the ipsilateral spinal dorsal horn in primates [10] thus, the main source of the NVR would be the spinal dorsal horn. Therefore, the spinal NVR reported here is probably generated mainly by sensory orthodromic stimulation of the dorsal horn interneurons and spread through the peri-spinal vascular network.

K. Future Work

Previous fNIRS applications were aimed to monitor indirectly the spinal cord perfusion/oxygenation status during

surgical procedures [48]. In contrast, our novel approach is aimed at a direct recording of the peri-spinal NVR triggered by a peripheral nerve electrical stimulation. Hence, it is useful for evaluating spinal sensory neuronal population activity, a key factor for the neurovascular coupling phenomena. Reduction on the SDH neuronal population due to traumatic, degenerative, or pharmacologic effects may reduce the spinal NVR, but increases in neuronal excitability i.e., neuropathic pain, probably will increase this response [13], [14] allowing its detection and quantification. Additionally, the fNIRS could monitor the spinal pharmacological response to non-steroidal anti-inflammatory drugs and/or evaluation of treatment approaches [28], [29], [48]. Potential diagnostic application of this method on spinal motor response should be tested, by increasing the intensity of the electrical stimulation to reach motor fiber threshold or by intense and/or long-lasting motor tasks, however, this approach requires handle motion artifacts and could activate the unspecific sympathetic skin response.

Further data is needed to evaluate spinal NVR to posterior tibialis nerve alone or combined to median nerve stimulation for orthodromic/antidromic protocols to get more physiological insight. Group-specific data such as by sex, age, or pathology i.e., diabetes, arterial hypertension, neuropathic pain, spinal cord injury, is needed for more clinically relevant data. In the present study, different experimental stimulation protocols were tested to characterize the spinal NVR by fNIRS which prolongs the individual test to around 30 minutes. It is probably that selection of the clinically relevant protocol will reduce this test time to less than 10 minutes, well shorter than a standard spine MRI test, and almost similar than an SSEP test.

Non-invasive NVR recording shows the potential application as a functional evaluation of the spinal cord. The potential use of this relatively low-cost, low maintenance, short test time and potentially mobile technology of fNIRS to obtain relevant functional insights would be a clear breakthrough in spinal cord monitoring. However, the fNIRS shows a lower spatial (anatomical) resolution compared to MRI due to intrinsic scattering of the near infrared light and spreading nature of the NVR. Additionally, the signal-to-noise ratio for a spinal response recorded by our fNIRS is better than that reported up to date for spinal fMRI.

Acknowledgment

The authors thank Dr. María Rodriguez Fernandez for providing part of the equipment (EMG), to Instituto de Ingenieria Biologica y Medica of the Pontificia Universidad Católica de Chile for the clinical location to perform the fNIRS recordings, and to Dr. Raúl Caulier for signal processing in some of the data. The author Sergio Uribe also thanks the Millennium Nucleus on Cardiovascular Magnetic Resonance of the Millennium Science Initiative from the National Agency for Research and Development (ANID).

References

[1] F. Biering-Sørensen and S. Kirshblum, "International perspectives on spinal cord injury," in *Spinal Cord Medicine*, 3rd ed. New York, NY, USA: Springer, 2018, pp. 1007–1022.

[2] M. C. Battié, T. Videman, and E. Parent, "Lumbar disc degeneration: Epidemiology and genetic influences," *Spine*, vol. 29, no. 23, pp. 2679–2690, Dec. 2004.

[3] S. Rajasekaran *et al.*, "The value of CT and MRI in the classification and surgical decision-making among spine surgeons in thoracolumbar spinal injuries," *Eur. Spine J.*, vol. 26, no. 5, pp. 1463–1469, May 2017.

[4] F. Scholkmann *et al.*, "A review on continuous wave functional near-infrared spectroscopy and imaging instrumentation and methodology," *Neuroimage*, vol. 85, no. 1, pp. 6–27, Jan. 2014.

[5] P. Nash *et al.*, "Functional magnetic resonance imaging identifies somatotopic organization of nociception in the human spinal cord," *Pain*, vol. 154, no. 6, pp. 776–781, 2013.

[6] G. Giulietti, F. Giove, G. Garreffa, C. Colonnese, S. Mangia, and B. Maraviglia, "Characterization of the functional response in the human spinal cord: Impulse-response function and linearity," *NeuroImage*, vol. 42, no. 2, pp. 626–634, Aug. 2008.

[7] W. H. Backes, W. H. Mess, and J. T. Wilmink, "Functional MR imaging of the cervical spinal cord by use of median nerve stimulation and fist clenching," *Amer. J. Neuroradiol.*, vol. 22, no. 10, pp. 1854–1859, 2001.

[8] N. Kinany, E. Pirondini, S. Micera, and D. Van De Ville, "Dynamic functional connectivity of resting-state spinal cord fMRI reveals fine-grained intrinsic architecture," *Neuron*, vol. 108, pp. 424–435, Nov. 2020.

[9] H. Islam, C. S. Law, K. A. Weber, S. C. Mackey, and G. H. Glover, "Dynamic per slice shimming for simultaneous brain and spinal cord fMRI," *Magn. Reson. Med.*, vol. 81, no. 2, pp. 825–838, 2019.

[10] T.-L. Wu *et al.*, "Intrinsic functional architecture of the non-human primate spinal cord derived from fMRI and electrophysiology," *Nature Commun.*, vol. 10, no. 1, pp. 1–10, Dec. 2019.

[11] K. A. Weber *et al.*, "Assessing the spatial distribution of cervical spinal cord activity during tactile stimulation of the upper extremity in humans with functional magnetic resonance imaging," *Neuroimage*, vol. 217, Aug. 2020, Art. no. 116905.

[12] J. Kimura, *Electrodiagnosis in Diseases of Nerve and Muscle: Principles and Practice*. London, U.K.: Oxford Univ. Press, 2013.

[13] W. D. Willis and R. E. Coggeshall, *Sensory Mechanisms of the Spinal Cord: Primary Afferent Neurons and the Spinal Dorsal Horn*, vol. 1. Boston, MA, USA: Springer, 2004.

[14] K. Shimoji, "Origins and properties of spinal cord evoked potentials," in *Atlas of Human Spinal Cord Evoked Potentials*. Washington, DC, USA: Butterworth, 1995, pp. 1–25.

[15] C. D. Etz *et al.*, "Near-infrared spectroscopy monitoring of the collateral network prior to, during, and after thoracoabdominal aortic repair: A pilot study," *Eur. J. Vascular Endovascular Surg.*, vol. 46, no. 6, pp. 651–656, Dec. 2013.

[16] D. T. Delpy, M. Cope, P. van der Zee, S. Arridge, S. Wray, and J. Wyatt, "Estimation of optical pathlength through tissue from direct time of flight measurement," *Phys. Med. Biol.*, vol. 33, no. 12, pp. 1433–1442, 1988.

[17] N. Naseer and K.-S. Hong, "fNIRS-based brain-computer interfaces: A review," *Frontiers Hum. Neurosci.*, vol. 9, p. 3, Jan. 2015.

[18] S. Sreedharan, R. Sitaram, J. S. Paul, and C. Kesavadas, "Brain-computer interfaces for neurorehabilitation," *Crit. Rev. Biomed. Eng.*, vol. 41, no. 3, pp. 269–279, 2013.

[19] B. Shadgan *et al.*, "Optical monitoring of spinal cord subcellular damage after acute spinal cord injury," *Proc. SPIE*, vol. 10501, Feb. 2018, Art. no. 105010L.

[20] F. I. Valenzuela, S. A. Uribe, A. Eblen-Zajjur, R. Sitaram, and M. Rana, "Device for recording the vascular response of the human spinal cord triggered by a suprasensible stimulus through the use of functional near-infrared spectroscopy," U.S. Patent 16 958 433, Feb. 25, 2021.

[21] L. Gagnon, R. J. Cooper, M. A. Yücel, K. L. Perdue, D. N. Greve, and D. A. Boas, "Short separation channel location impacts the performance of short channel regression in NIRS," *Neuroimage*, vol. 59, no. 3, pp. 2518–2528, Feb. 2012.

[22] A. A. Eblen-Zajjur and J. Sandkühler, "Synchronicity of nociceptive and non-nociceptive adjacent neurons in the spinal dorsal horn of the rat: Stimulus-induced plasticity," *Neuroscience*, vol. 76, no. 1, pp. 39–54, Dec. 1996.

[23] E. Contreras-Hernández, D. Chávez, and P. Rudomin, "Dynamic synchronization of ongoing neuronal activity across spinal segments regulates sensory information flow," *J. Physiol.*, vol. 593, no. 10, pp. 2343–2363, May 2015.

[24] J. Meléndez-Gallardo and A. Eblen-Zajjur, "Noxious mechanical heterotopic stimulation induces inhibition of the spinal dorsal horn neuronal network: Analysis of spinal somatosensory-evoked potentials," *Neurolog. Sci.*, vol. 37, no. 9, pp. 1491–1497, Sep. 2016.

[25] C. J. Anderson, D. N. Anderson, S. M. Pulst, C. R. Butson, and A. D. Dorval, "Neural selectivity, efficiency, and dose equivalence in deep brain stimulation through pulse width tuning and segmented electrodes," *Brain Stimul.*, vol. 13, no. 4, pp. 1040–1050, Jul. 2020.

[26] J. Glykys, M. Guadama, L. Marcano, E. Ochoa, and A. Eblen-Zajjur, "Inflammation induced increase of fluoride resistant acid phosphatase (FRAP) activity in the spinal dorsal horn in rats," *Neurosci. Lett.*, vol. 337, no. 3, pp. 167–169, Feb. 2003.

[27] M. Czaplinski, C. Abad, and A. Eblen-Zajjur, "Normal expression and inflammation-induced changes of Na and Na/K ATPase activity in spinal dorsal horn of the rat," *Neurosci. Lett.*, vol. 374, no. 2, pp. 147–151, Feb. 2005.

[28] J. A. Filosa, H. W. Morrison, J. A. Iddings, W. Du, and K. J. Kim, "Beyond neurovascular coupling, role of astrocytes in the regulation of vascular tone," *Neuroscience*, vol. 323, pp. 96–109, May 2016.

[29] S. Tarantini, C. H. T. Tran, G. R. Gordon, Z. Ungvari, and A. Csiszar, "Impaired neurovascular coupling in aging and Alzheimer's disease: Contribution of astrocyte dysfunction and endothelial impairment to cognitive decline," *Exp. Gerontol.*, vol. 94, pp. 52–58, Aug. 2017.

[30] H. Vanegas and H.-G. Schaible, "Prostaglandins and cycloxygenases in the spinal cord," *Prog. Neurobiol.*, vol. 64, no. 4, pp. 327–363, Jul. 2001.

[31] X. F. Figueroa and B. R. Duling, "Gap junctions in the control of vascular function," *Antioxidants Redox Signaling*, vol. 11, no. 2, pp. 251–266, Feb. 2009.

[32] C. de Wit and T. M. Griffith, "Connexins and gap junctions in the EDHF phenomenon and conducted vasomotor responses," *Pflügers Arch. Eur. J. Physiol.*, vol. 459, no. 6, pp. 897–914, May 2010.

[33] B. R. Chen, M. G. Kozberg, M. B. Bouchard, M. A. Shaik, and E. M. C. Hillman, "A critical role for the vascular endothelium in functional neurovascular coupling in the brain," *J. Amer. Heart Assoc.*, vol. 3, no. 3, pp. 1–14, May 2014.

[34] G. E. Strangman, Z. Li, and Q. Zhang, "Depth sensitivity and source-detector separations for near infrared spectroscopy based on the Colin27 brain template," *PLoS ONE*, vol. 8, no. 8, Aug. 2013, Art. no. e66319.

[35] M. A. Yücel, C. M. Aasted, M. P. Petkov, D. Borsook, D. A. Boas, and L. Becerra, "Specificity of hemodynamic brain responses to painful stimuli: A functional near-infrared spectroscopy study," *Sci. Rep.*, vol. 5, no. 1, pp. 1–9, Aug. 2015.

[36] H. Toda, H. Maruyama, B. Budgell, and M. Kurosawa, "Responses of dorsal spinal cord blood flow to noxious mechanical stimulation of the skin in anesthetized rats," *J. Physiolog. Sci.*, vol. 58, no. 4, pp. 263–270, 2008.

[37] M. Piché, T. Paquette, and H. Leblond, "Tight neurovascular coupling in the spinal cord during nociceptive stimulation in intact and spinal rats," *Neuroscience*, vol. 355, pp. 1–8, Jul. 2017.

[38] J. Sandkühler, B. Stelzer, and Q.-G. Fu, "Characteristics of propriospinal modulation of nociceptive lumbar spinal dorsal horn neurons in the cat," *Neuroscience*, vol. 54, no. 4, pp. 957–967, Jun. 1993.

[39] H. Vanegas and H.-G. Schaible, "Descending control of persistent pain: Inhibitory or facilitatory?" *Brain Res. Rev.*, vol. 46, no. 3, pp. 295–309, Nov. 2004.

[40] M. H. Ossipov, G. O. Dussor, and F. Porreca, "Central modulation of pain," *J. Clin. Invest.*, vol. 120, no. 11, pp. 3779–3787, 2010.

[41] M. Chagín-Nazar and A. Eblen-Zajjur, "Effect of noxious Bucal trigeminal high frequency electrical stimulation on lumbar spinal cord evaluated by evoked potentials in the rat," *Arch. Neurociencias*, vol. 20, no. 4, pp. 258–264, 2015.

[42] F. Ramírez and H. Vanegas, "Tooth pulp stimulation advances both medullary off-cell pause and tail flick," *Neurosci. Lett.*, vol. 100, nos. 1–3, pp. 153–156, May 1989.

[43] P. W. Stroman *et al.*, "The current state-of-the-art of spinal cord imaging: Methods," *Neuroimage*, vol. 84, pp. 1070–1081, Jan. 2014.

[44] J. Sandkühler, A. Eblen-Zajjur, Q.-G. Fu, and C. Forster, "Differential effects of spinalization on discharge patterns and discharge rates of simultaneously recorded nociceptive and non-nociceptive spinal dorsal horn neurons," *Pain*, vol. 60, no. 1, pp. 55–65, 1995.

[45] J. Sandkühler, J. G. Chen, G. Cheng, and M. Randić, "Low-frequency stimulation of afferent Aδ-fibers induces long-term depression at primary afferent synapses with substantia gelatinosa neurons in the rat," *J. Neurosci.*, vol. 17, no. 16, pp. 6483–6491, Aug. 1997.

[46] J. E. Beall, A. E. Applebaum, R. D. Foreman, and W. D. Willis, "Spinal cord potentials evoked by cutaneous afferents in the monkey," *J. Neurophysiol.*, vol. 40, no. 2, pp. 199–211, Mar. 1977.

[47] O. U. Scremin and E. E. Decima, "Control of blood flow in the cat spinal cord," *J. Neurosurg.*, vol. 58, no. 5, pp. 742–748, May 1983.

[48] R. Sitaram *et al.*, "Closed-loop brain training: The science of neurofeedback," *Nat. Rev. Neurosci.*, vol. 18, no. 2, pp. 86–100, 2017.